

3.3 NUMERICAL RESULTS AND DISCUSSION

The damping expressions for the magnetic wiggler fields and the electric wiggler fields are plotted to demonstrate their dependence on ω_p and ω_b . The damping expressions for the newly created electromagnetic waves having frequencies ω_1 through ω_4 are also plotted versus ω_p and ω_b for reference.

The damping terms are incorporated into the wiggler field equations and plotted. Letting $\omega_{bw} = 0$ in equation (2.3) corresponds to having no incident wiggler magnetic field and is referred to as the isotropic case. In this case, equation (2.27) shows that a magnetic wiggler field is still created. The helical magnetic wiggler created has a purely circular cross section. This is referred to as case 1.

Letting $k_w \approx 0$ and $\phi_w = \frac{\pi}{2}$ in equation (2.3) corresponds to an incident field similar to that discussed in [8]. Examination of equation (2.27) shows that the created helical magnetic wiggler field has an elliptical cross section. In order to better compare this case to case 1, a value for p in equation (2.1) is chosen to result in a helical magnetic wiggler field with nearly circular cross section. This is found by setting the x and y components equal to each other. The expression for p for this case is found to be

$$p = \frac{\omega_p^4 + \omega_o^2(\omega_{bw}^2 \sin(k_w z + \phi_w) + \omega_p^2)}{\omega_p^2(\omega_o^2 + \omega_p^2)} \quad (3.8)$$

$$p = \left[\frac{\omega_p^4 + \omega_o^2(\omega_{bw}^2 + \omega_p^2)}{\omega_p^2(\omega_o^2 + \omega_p^2)} \right]_{k_w=0, \phi_w=\frac{\pi}{2}} \quad (3.9)$$

This is referred to as case 2.

Introducing the damping terms in (2.25b) and (2.26b) into (2.27) and letting $r = 1$ we have the following for each case:

Case 1:

$$\frac{\overrightarrow{h_w(z)}}{H_o} = \hat{y} p \frac{\left(\frac{\omega_p}{\omega_o}\right)^2 \cos\left(2\pi\frac{z}{\lambda_o}\right)}{1 + \left(\frac{\omega_p}{\omega_o}\right)^2} e^{-(1)\sigma_w o} \pm \hat{x} q \frac{\left(\frac{\omega_p}{\omega_o}\right)^2 \sin\left(2\pi\frac{z}{\lambda_o}\right)}{1 + \left(\frac{\omega_p}{\omega_o}\right)^2} e^{-(1)\sigma_w o} \quad (3.10)$$

where we let $p = 1$ and $q = 1$.

Case 2:

$$\frac{\overrightarrow{h_w(z)}}{H_o} = \hat{y} p \frac{\left(\frac{\omega_p}{\omega_o}\right)^4 \cos\left(2\pi\frac{z}{\lambda_o}\right)}{\left(\frac{\omega_p}{\omega_o}\right)^4 + \left(\frac{\omega_{bw}}{\omega_o}\right)^2 \sin^2\left(2\pi\frac{k_w}{k_o}\frac{z}{\lambda_o} + \phi_w\right) + \left(\frac{\omega_p}{\omega_o}\right)^2} e^{-(1)\sigma_w x} \pm \hat{x} q \frac{\left(\frac{\omega_p}{\omega_o}\right)^2 \sin\left(2\pi\frac{z}{\lambda_o}\right)}{1 + \left(\frac{\omega_p}{\omega_o}\right)^2} e^{-(1)\sigma_w o} \quad (3.11)$$

where we have p as in (3.2).

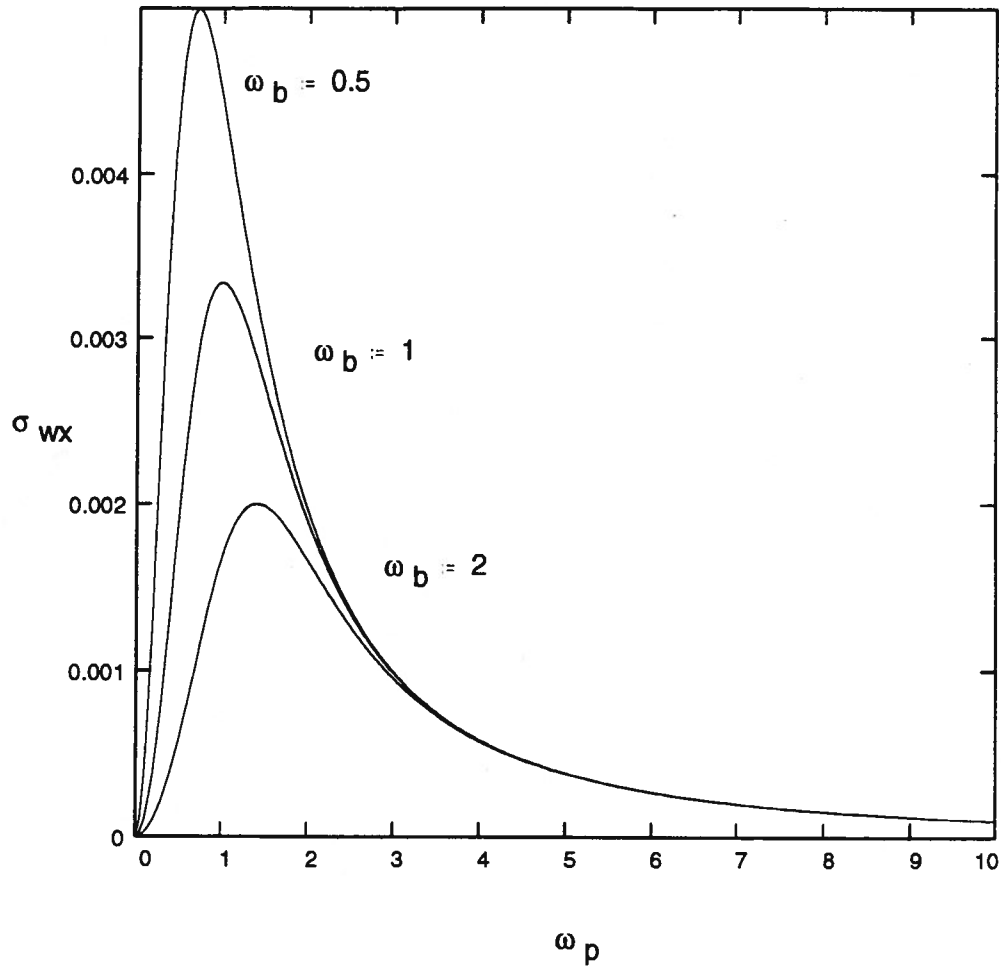


Figure. 3.1 Damping of the y component of the magnetic wiggler field and the electric wiggler field vs. ω_p

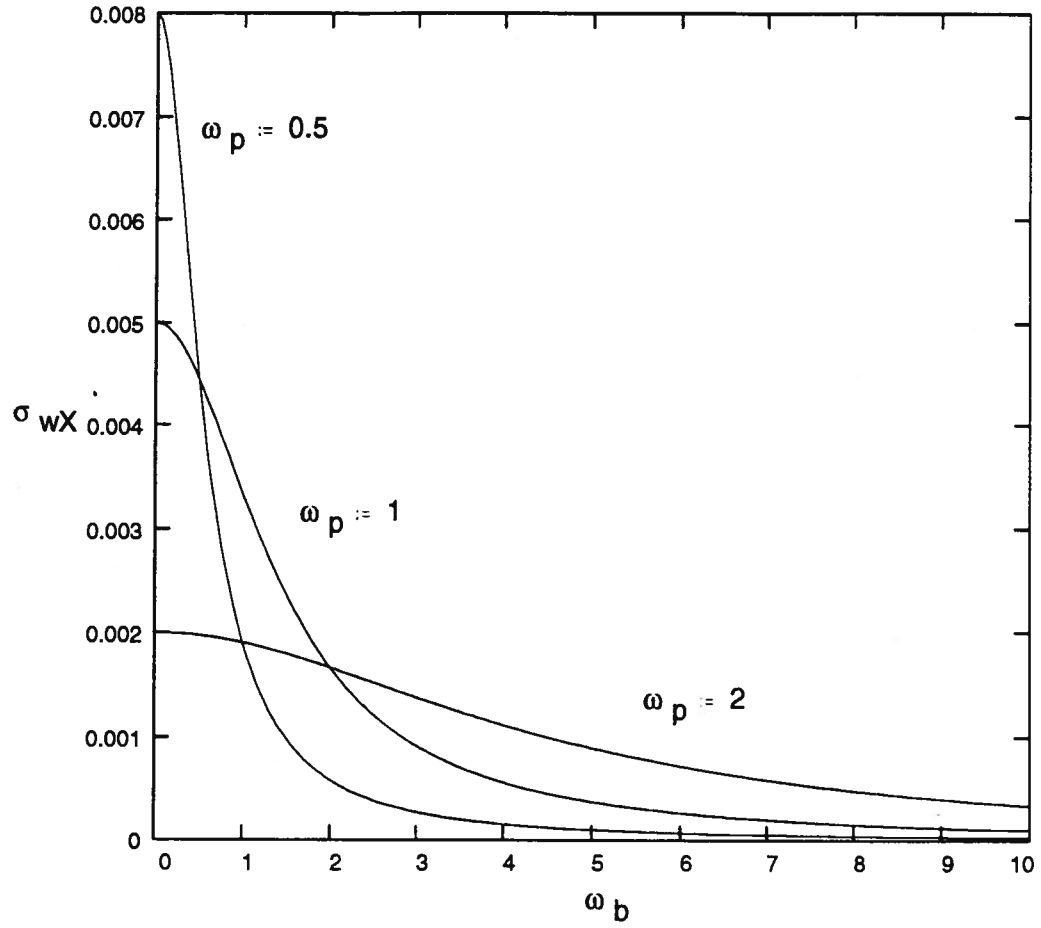


Figure 3.2 Damping of the y component of the magnetic wiggler field and the electric wiggler field vs. ω_b

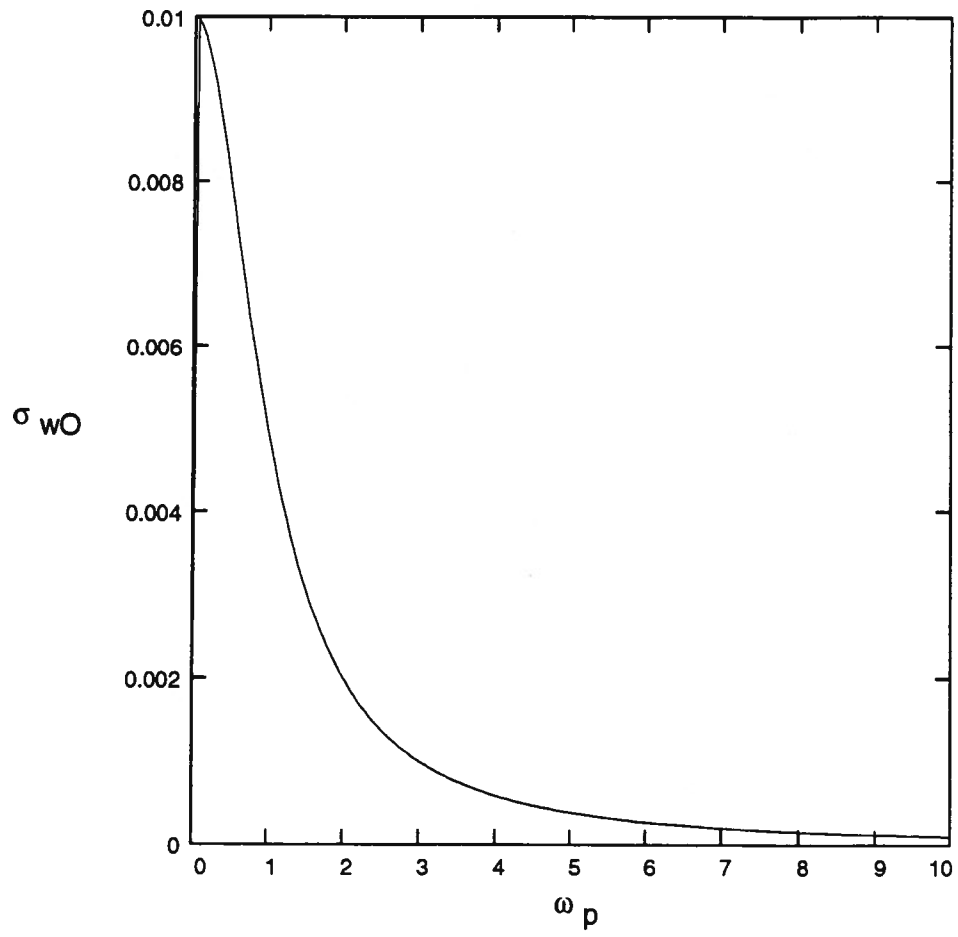


Figure 3.3 Damping of the x component of the magnetic wiggler field vs. ω_p .

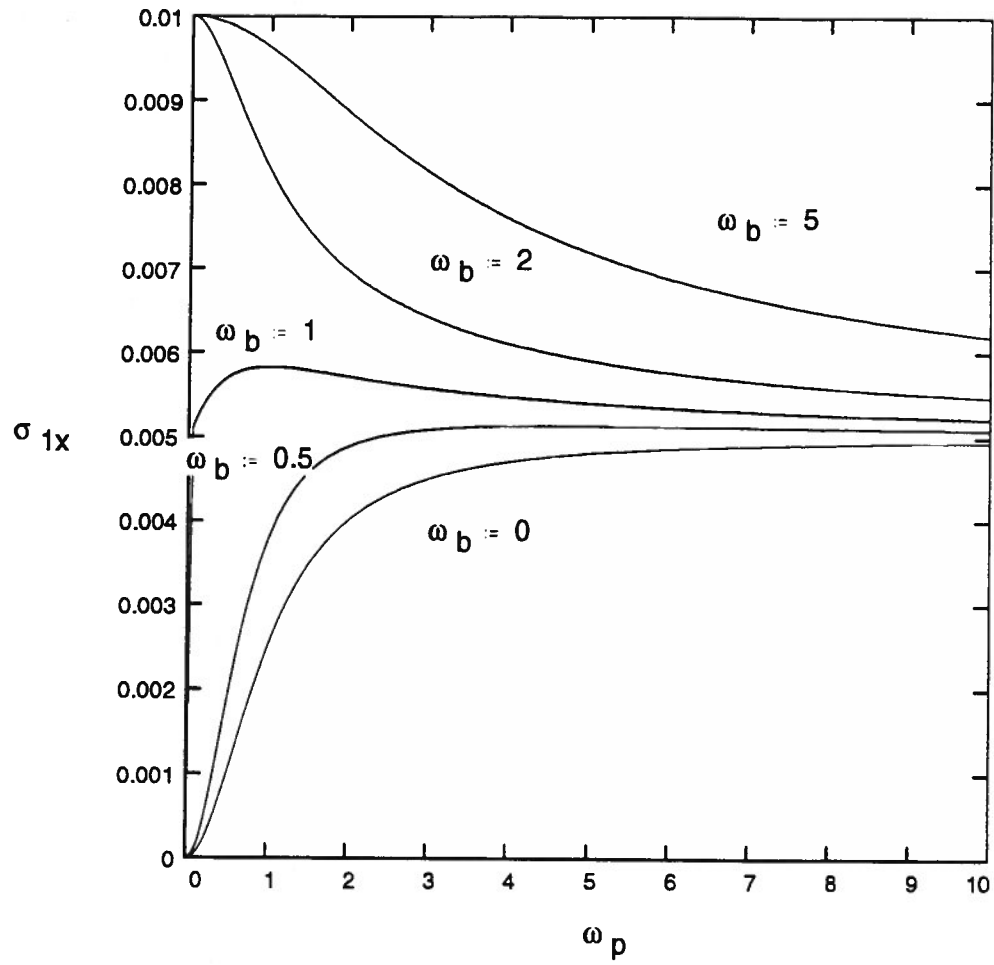


Figure 3.4 Damping of the newly created waves associated with the frequency ω_1 vs. ω_p .

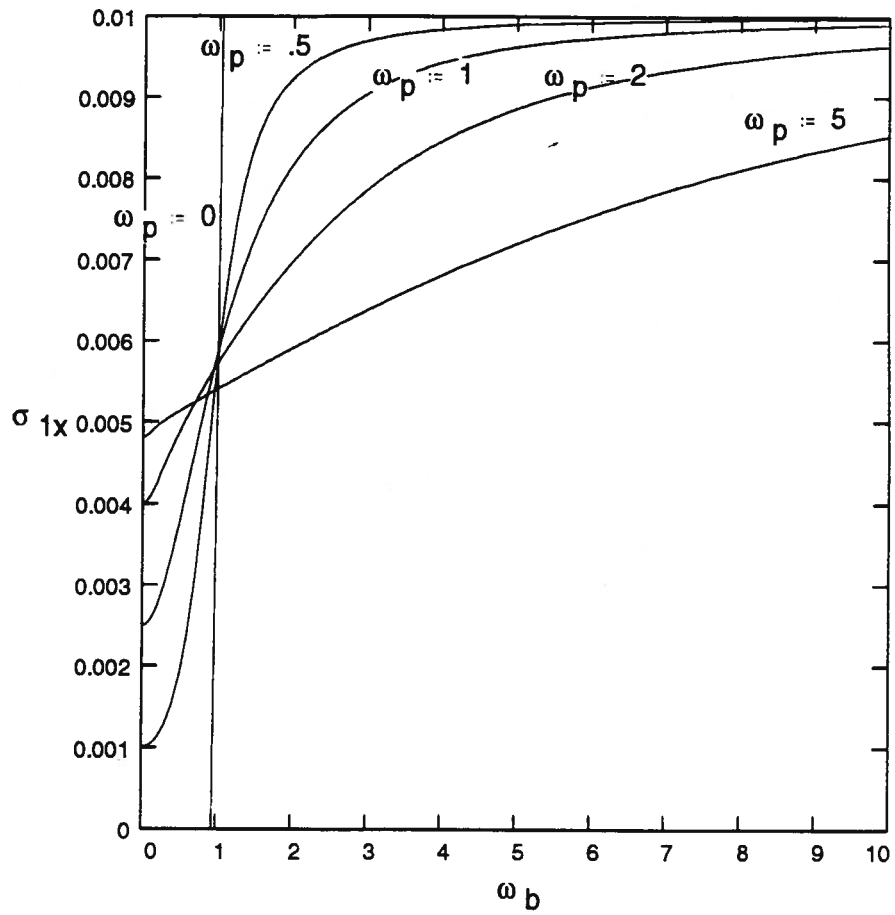


Figure 3.5 Damping of the newly created waves associated with the frequency ω_1 vs. ω_b .

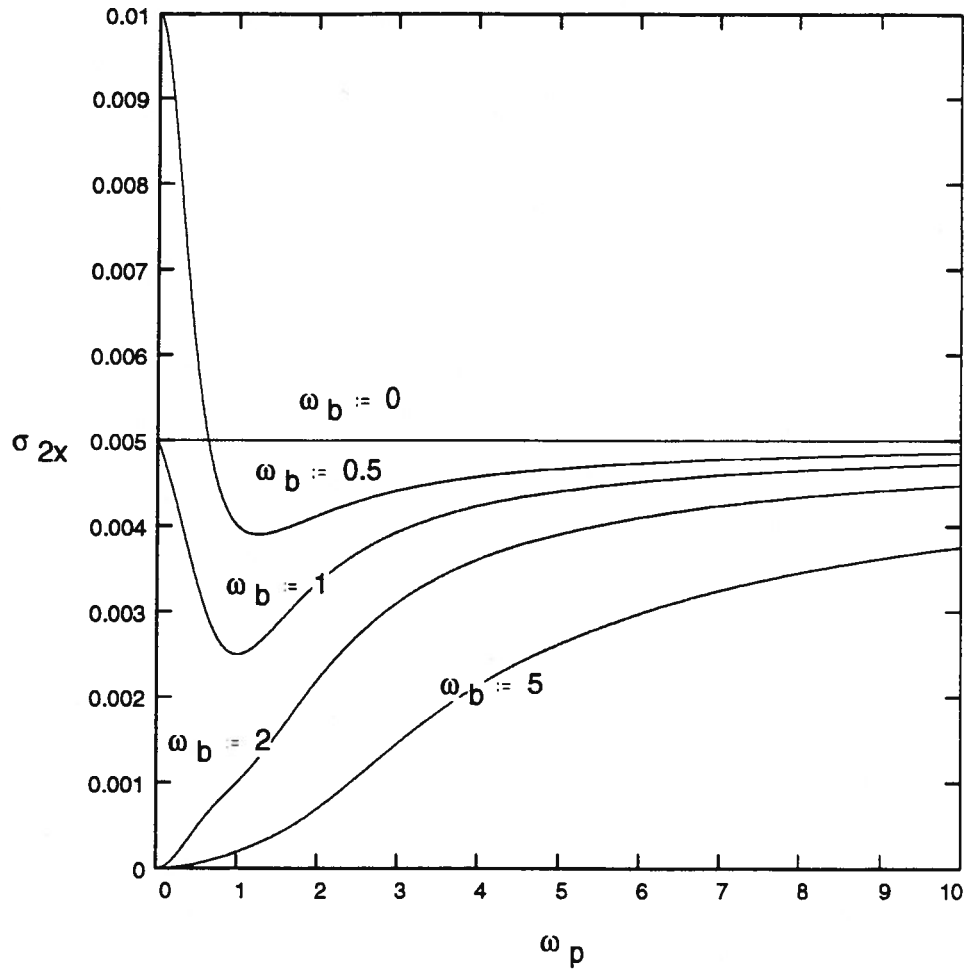


Figure 3.6 Damping of the newly created waves associated with the frequency ω_2 vs. ω_p .

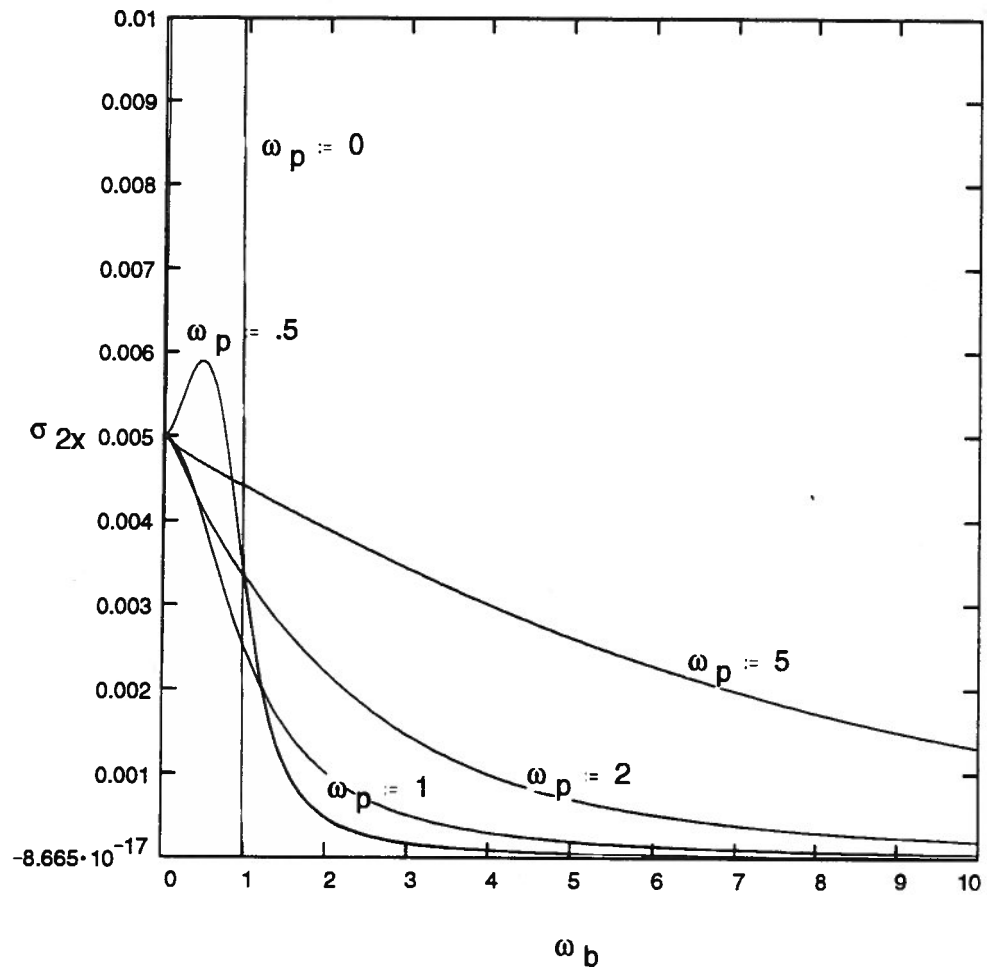


Figure 3.7 Damping of the newly created waves associated with the frequency ω_2 VS. ω_b .

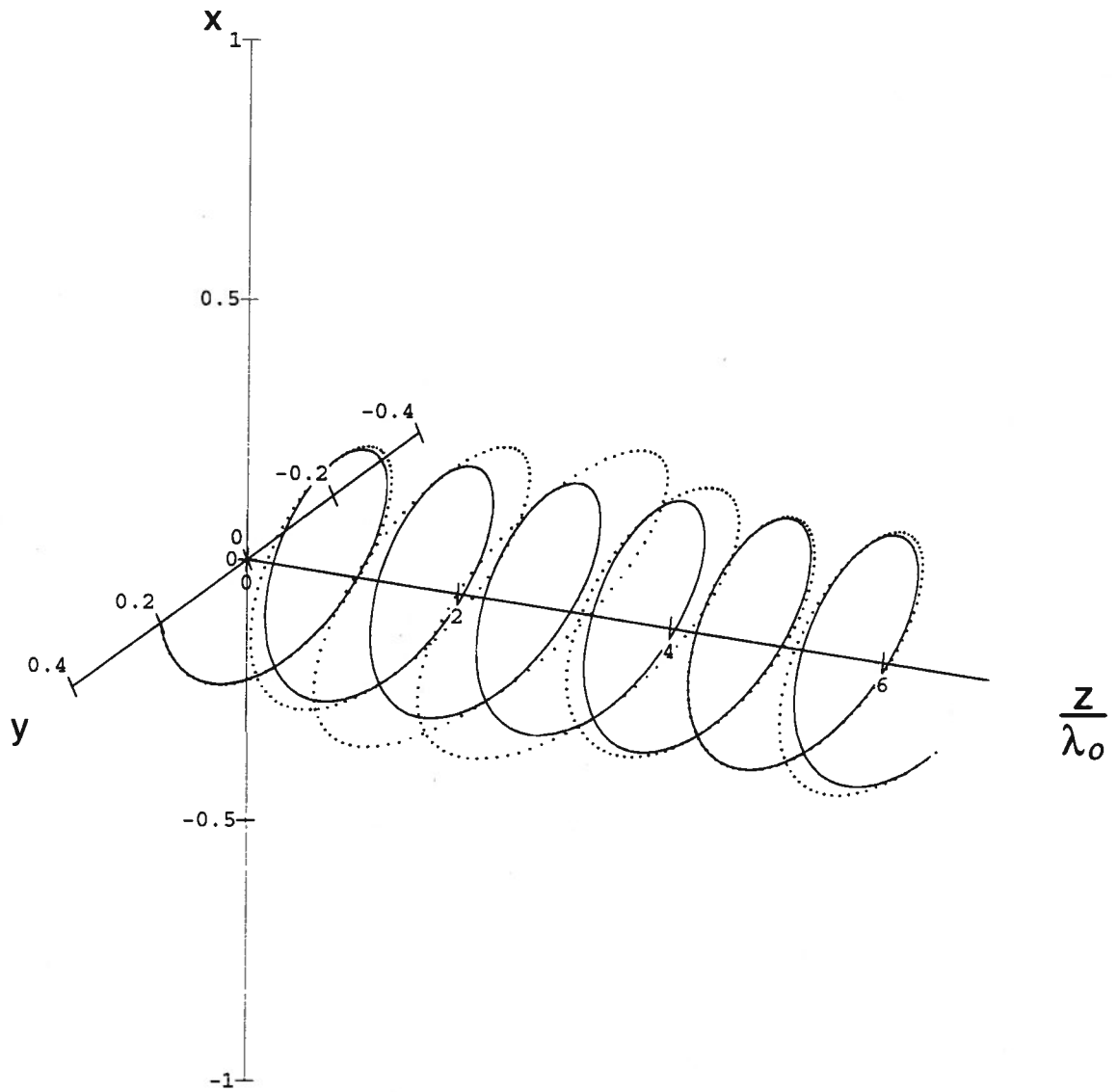


Figure 3.8 Comparison of the damping of the magnetic wiggler field produced in the isotropic case vs. the anisotropic case.